Table S1. Numbers of samples for each category of MCSs and their proportion to the total number of samples, which are categorized by fitting curves using sixth-order (a) and fourth-order (b) polynomial. Note that all the samples (from MCS Type a-d) used for statistics meet the requirements that the goodness of fit (R_a^2) of both the minimum BT and the equivalent radius higher than or equal to 0.6.

(a)

	MCS					
	Type-a	**Type-b**	**Type-c**	**Type-d**	**Type-e**	**Type-f**
# of verified trajectories of MCS	1714	1475	526	1574	306	92
Percentage (%)	30.14	25.94	9.25	27.68	5.38	1.62

(b)

	MCS					
	Type-a	**Type-b**	**Type-c**	**Type-d**	**Type-e**	**Type-f**
# of verified trajectories of MCS	1602	1218	349	1466	207	57
Percentage (%)	32.70	24.86	7.12	29.92	4.23	1.16

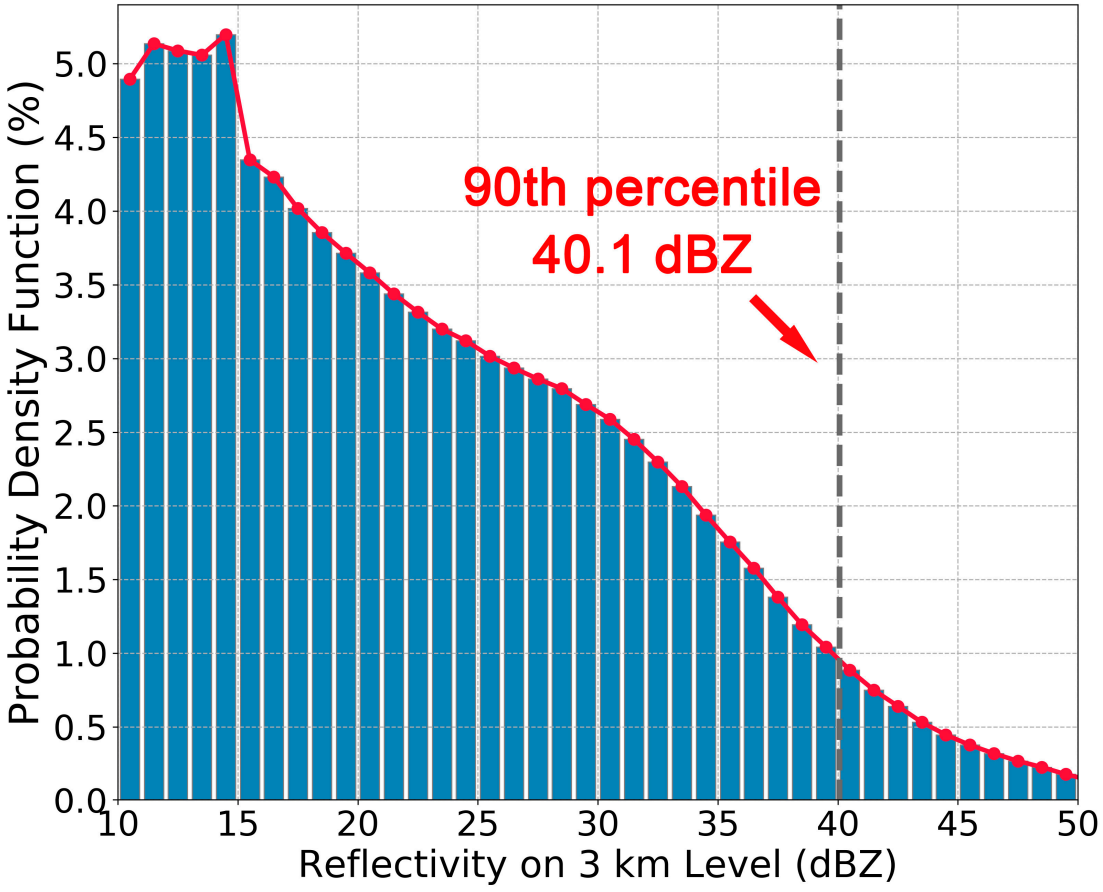

Figure S1. Bars showing the probability density function of radar reflectivity at 3 km above sea level. The grey dashed line denotes 90th percentile of the reflectivity. Note that only the reflectivity higher than or equal to 10 dBZ is used for statistics here.

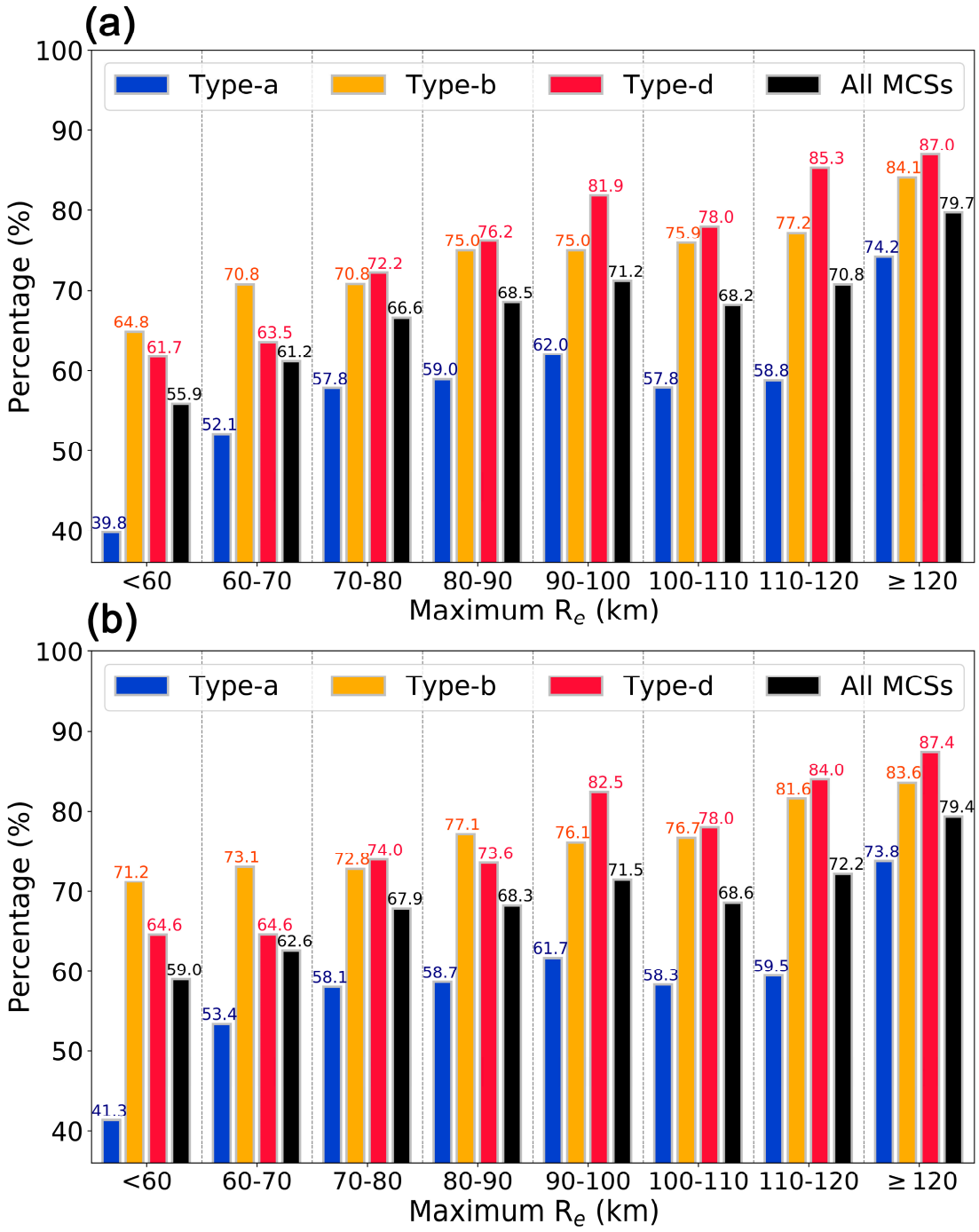

Figure S2. Same as Figure 5a, but for the thresholds of BT_{edge} chosen as 240 K (a) and 260 K (b).

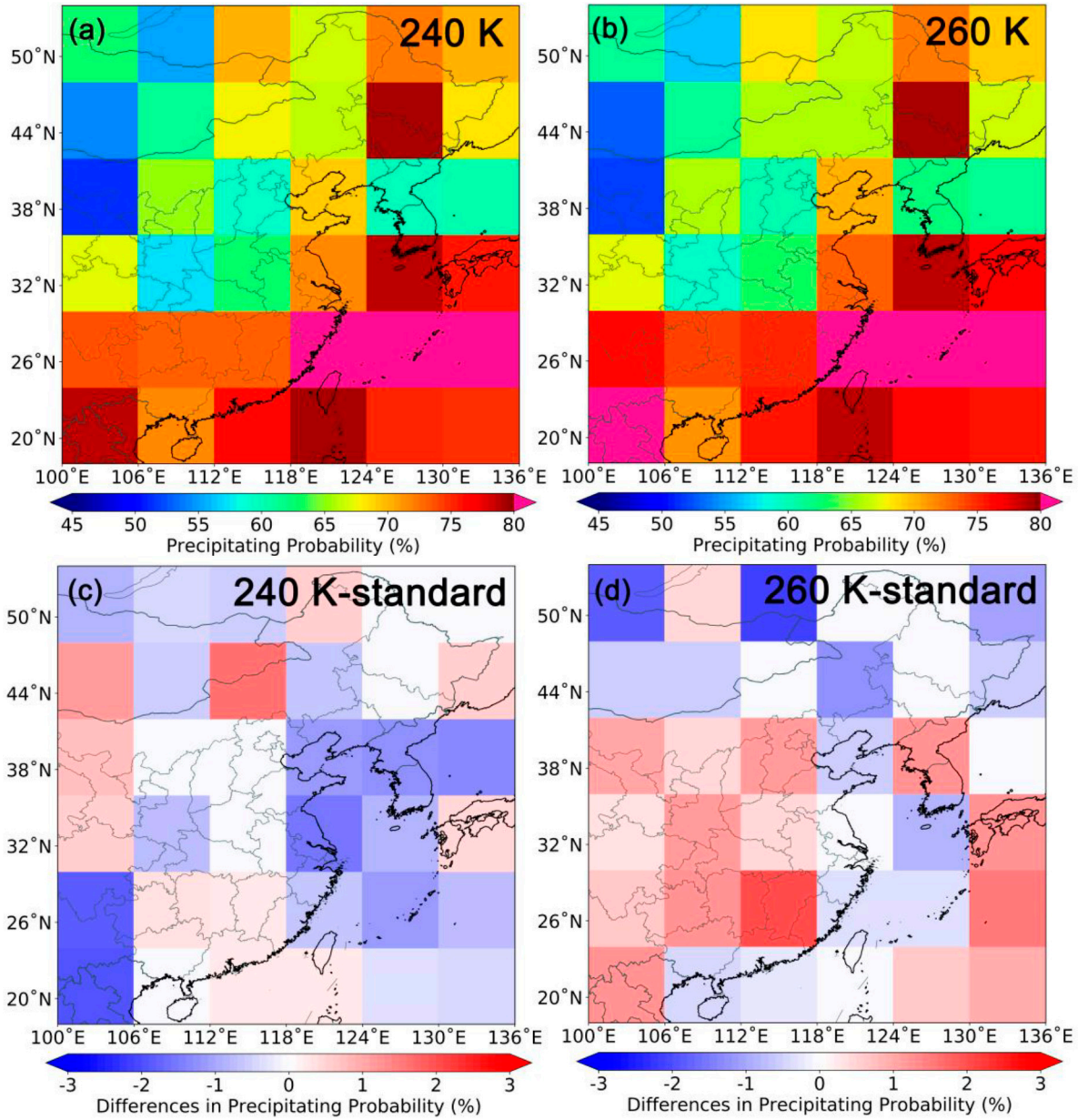

Figure S3. Same as Figure 5b, but for the thresholds of BT_{edge} chosen as 240 K (a) and 260 K (b). The two panels in the bottom denote the differences in precipitation probability between 240 K (c)/260 K (d) and standard value of BT_{edge}, respectively.

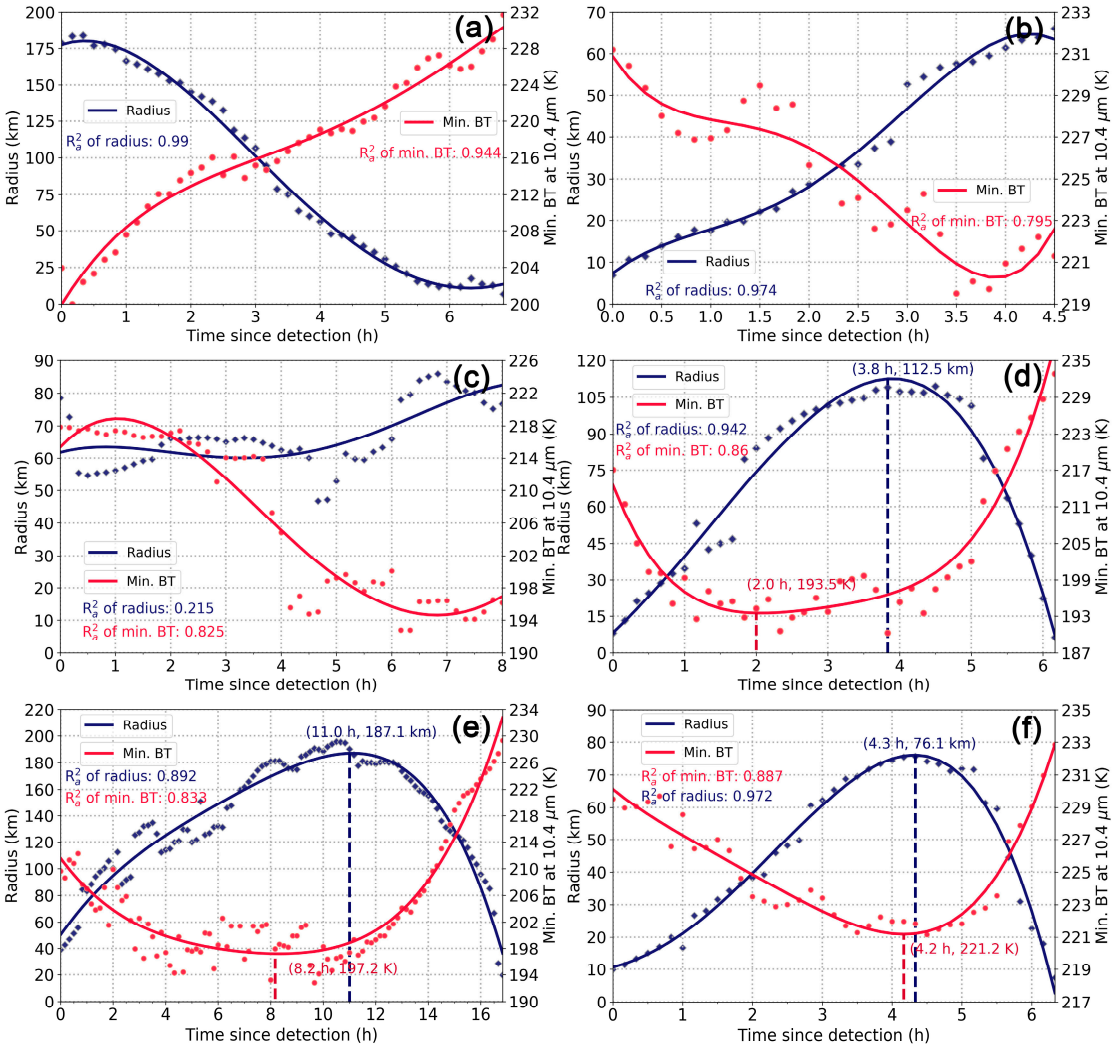

Figure S4. Same as Figure 4, but using fourth-order polynomial when fitting the observations by AHI.

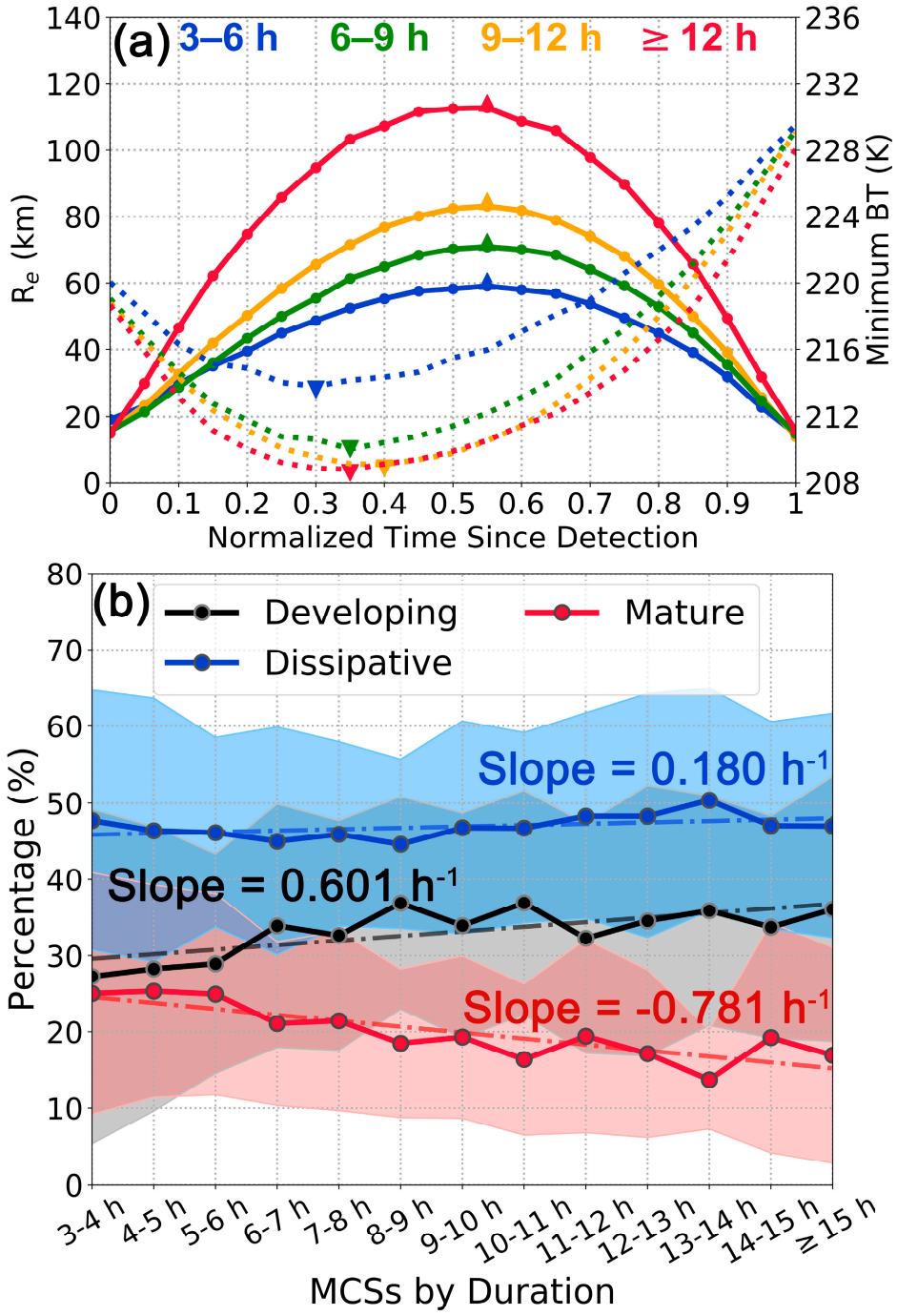

Figure S5. Same as Figs. 6a, 6c, but using fourth-order polynomial when fitting the observations by AHI.